In Vivo Testing of a Miniature 2.4 / 4.8 GHz Implantable Antenna in Post Mortem Human Subject

John Blauert, *Student Member, IEEE*, Yun-Seok Kang, and Asimina Kiourti, *Member, IEEE*

Abstract— We present a novel miniaturized dual-band implantable antenna for microwave backscattering at 2.4/4.8 GHz. These bands are recently emerging as highly promising for batteryless implants, viz. implants that receive power from an exterior interrogator at 2.4 GHz and backscatter their sensed signals at 4.8 GHz. Compared to the smallest reported 2.4/4.8 GHz implantable antenna, the proposed design is miniaturized by 39%, and exhibits higher gain by 10.3 dB (at 2.4 GHz) and 2.6 dB (at 4.8 GHz). To validate the antenna performance under anatomically correct conditions, post mortem human subject (PMHS) testing is performed. To our knowledge, this is the first time that implantable antennas are tested in PMHS and further compared vs. simulations in tissue-emulating models. Notably, good agreement exists between the two, with the proposed antenna exhibiting a reflection coefficient of < -4.5 dB at both 2.4 and 4.8 GHz for all six subcutaneous locations measured: left/right sides of thigh, hip, and abdomen.

Index Terms— Biomedical telemetry, harmonic backscattering, implantable antennas, *in vivo* testing, wireless implants.

I. INTRODUCTION

WIRELESS implants (brain sensors, glucose monitors, etc.) [1]-[3] can dramatically improve the quality of healthcare by providing round-the-clock monitoring of deep tissue vitals. Numerous implantable antennas have been designed to allow for communication links to be wireless [4]-[18]. One of the major challenges associated with wireless implants relates to the way of powering them. Batteries are typically employed, but they are bulky and require frequent replacement/recharging. Enabling batteryless operation would help improve the implants' unobtrusiveness and long-term stability. One way to achieve this goal is through microwave harmonic backscattering [4]-[6].

J. Blauert and A. Kiourti are with the ElectroScience Laboratory, Dept. of Electrical and Computer Engineering, The Ohio State University, Columbus, OH, USA (e-mail: blauert.1@osu.edu, kiourti.1@osu.edu).
Y.-S. Kang is with the School of Health and Rehabilitation Sciences, The Ohio State University, Columbus, OH, USA.

Microwave harmonic backscattering allows for batteryless communication between an exterior (e.g., wearable) interrogating antenna and an implanted antenna in 3 steps: 1) the interrogating antenna transmits a fundamental frequency to an implanted antenna, 2) the implant receives the signal and mixes it with a biological signal (such as a neuropotential), and 3) the implant backscatters the harmonic mixed with the biological signal back to the interrogating antenna [4]-[6]. Expectedly, this technique necessitates the design of antennas that can radiate at both a fundamental frequency as well as the harmonic of said fundamental frequency. The Industrial, Scientific and Medical (ISM) band of 2.4-2.5 GHz is a natural choice for implanted medical devices [19]. Hence, microwave backscattering approaches reported to date for batteryless implants have used the 2.4/4.8 GHz bands [4]-[6].

Nevertheless, state-of-the-art implantable antennas for dual-band operation at 2.4/4.8 GHz exhibit relatively large footprints and/or low values of realized gain. Indeed, Table I compares the performance of previously reported 2.4/4.8 GHz implantable antennas vs. the proposed design (an identical 2 mm-deep subcutaneous implantation scenario is assumed in all cases). As seen, the smallest 2.4/4.8 GHz implantable antenna reported to date exhibits a footprint of 87 mm^2 and low broadside realized gains of -27 dB (at 2.4 GHz) and -14.6 dB (at 4.8 GHz) [6], stemming from poor matching at resonances. By contrast, antennas [4]-[5] offer higher realized gain, but utilize over 400% more surface area than this work, which is highly undesirable for implantation.

In this Letter, we propose a novel 2.4/4.8 GHz antenna that, compared to the smallest previous design [6], exhibits: a) a 39% decrease in footprint, and b) higher gain by 10.3 dB (at 2.4 GHz) and 2.6 dB (at 4.8 GHz). To test the antenna under anatomically correct conditions, the fabricated prototype is implanted in six subcutaneous locations (left/right sides of thigh, hip, and abdomen) of a post mortem human subject (PMHS). Measurement results are further compared with Finite Element (FE) simulations in multi-layer tissue models, showing good agreement. To our knowledge, this is the first time that implantable antennas are validated in PMHSs. Testing implanted antennas is commonly performed via tissue-emulating phantoms [15] or animal testing [16]. However, none of these approaches accurately emulate the human body anatomy. By contrast, our study is the first to demonstrate the feasibility of PMHS testing in implantable antenna design and

TABLE I. COMPARISON OF STATE-OF-THE-ART 2.4/4.8 GHz IMPLANTABLE ANTENNAS VS. THE PROPOSED DESIGN AT 2 MM IMPLANTATION DEPTH

| Ref.	Broadside Realized Gain (2.4 / 4.8 GHz)	Substrate Material	Antenna Type	Antenna Footprint
[4]	-16.2 / -2.67 dB	FR-4 (ε_r =4.6)	E-shaped Patch	15 mm × 15 mm (225 mm^2)
[5]	-14.8 / -4.41 dB	FR-4 (ε_r =4.6)	E-shaped patch with meandering arms	15mm × 16 mm (240 mm^2)
[6]	-27.0 / -14.6 dB	TMM 13i (ε_r =12.85)	E-shaped patch with meandering arms and a higher permittivity dielectric	8.7 × 10 mm^2 (87 mm^2)
This work	-16.7 / -12.0 dB	TMM 13i (ε_r =12.85)	E-shaped patch with meandering arms, higher permittivity dielectric and shorting pin	7.7 × 6.9 mm^2 (53.13 mm^2)

(a)   (b)
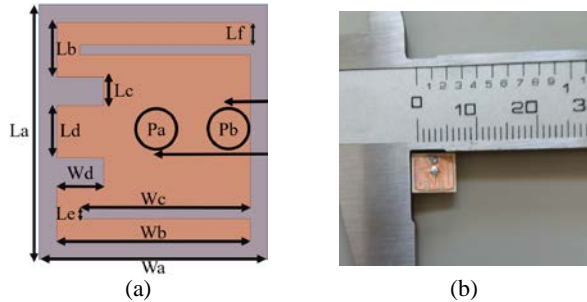
Fig. 1. Proposed 2.4/4.8 GHz implantable antenna: (a) model with dimensions shown in Table II, and (b) fabricated prototype.

TABLE II. DIMENSIONS OF THE PROPOSED IMPLANTABLE ANTENNA

Parameter	Value	Parameter	Value
La	7.7 mm	Wa	6.9 mm
Lb	1.7 mm	Wb	5.8 mm
Lc	0.9 mm	Wc	5.1 mm
Ld	1.6 mm	Wd	1.4 mm
Le	0.3 mm	Pa	3.4 mm
Lf	0.7 mm	Pb	1.1 mm

its potential to quantify detuning related to anatomical- and/or surgery-specific variations.

II. ANTENNA DESIGN

The proposed implantable antenna is shown in Fig. 1 with design parameters given in Table II. The antenna employs a miniaturized patch design, maintaining a volume of 7.7 × 6.9 × 1.52 mm^3. This offers a 39% reduction in surface area as compared to the previously smallest 2.4/4.8 GHz design [6]. This was accomplished by a) fabricating the antenna on a high permittivity substrate (TMM 13i, ε_r =12.85 and tanδ = 0.0019), b) meandering the arms to increase their electrical length, and c) including a shorting pin (at point Pb shown in Fig. 1). The shorting pin is primarily used to increase the effective size of the antenna, miniaturizing, in turn, its physical dimensions. This miniaturization technique acts much the same way as a ground plane doubles the height of a monopole antenna in [20]. The antenna is excited with a 50 Ω UFL connector on the ground plane and a 1 mm diameter via connecting it to the conducting plane at point Pa. To ensure biocompatibility, the antenna is coated with a 0.4 mm layer of polydimethylsiloxane (PDMS, ε_r =2.8 and tanδ = 0.001) [21]. Current densities are plotted in Fig. 2. The 2.4 GHz resonance

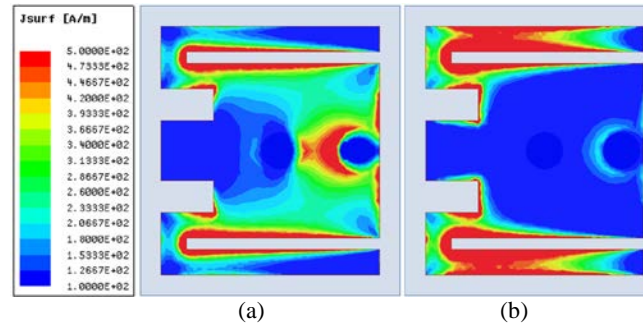(a)   (b)

Fig. 2. Simulated current densities of the implantable antenna at (a) 2.4 GHz, and (b) 4.8 GHz.

is developed from current flowing to the grounding via and around the meandering arm, whereas the 4.8 GHz resonance is primarily developed from the meandering arms.

III. SIMULATIONS

A. Simulation Set-Up

Finite Element (FE) simulations were carried out in Ansys High Frequency Structure Simulator (HFSS). As shown in Fig. 3, the antenna was placed right under the skin layer of a 3-layer rectangular tissue model, exhibiting a 2-mm-thick skin layer, an 8-mm-thick fat layer, and a 10-mm-thick muscle layer. Similar skin/fat thicknesses and implantation depths are reported in [4]-[6], [17]-[18]. The primary consideration of antenna design is the skin thickness as noted in [17]. The properties of the aforementioned tissues are laid out in Table III for both frequency bands of interest [22], [23].

B. Simulation Results

Antenna design was optimized for maximum realized gain at 2.4 GHz and 4.8 GHz. All antenna design parameters were parameterized, with the goals being: a) an overall footprint of smaller than [6], and b) broadside realized gain values higher than [5] for each of the bands. Indeed, as shown in Fig. 4, the final design exhibits broadside realized gain values of -16.7 dB (at 2.4 GHz) and -12.0 dB (at 4.8 GHz), which is 10.3 dB and 2.6 dB higher than [6], respectively. This occurs because the antenna has better matching and better directivity/beam shape than the previously designed antennas, thus exhibiting improved realized gain. Concurrently, the antenna footprint is 39% smaller than [6].

The reflection coefficient ($|S_{11}|$) of the proposed implantable antenna as a function of frequency is shown in Fig. 5. As seen, the antenna is well-matched at the target frequencies of 2.4
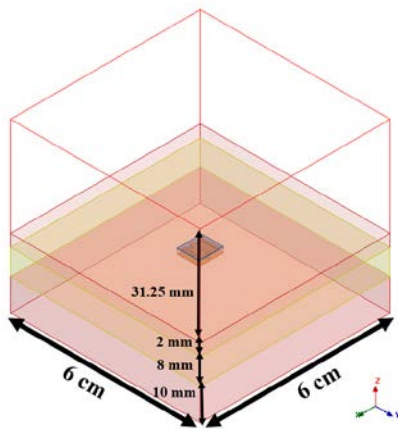
Fig. 3. Simulation set-up used to design the proposed antenna, which is placed directly under the 2mm skin layer.

TABLE III. PROPERTIES OF HUMAN TISSUE AT 2.4/4.8 GHz [21], [22]

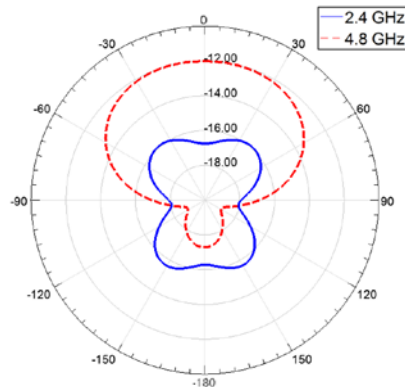| Property (2.4/4.8 GHz)	Skin	Fat	Muscle
ε_r	38.1 / 35.9	5.29 / 5.05	52.8 / 49.8
σ (S/m)	1.44 / 2.91	0.10 / 0.23	1.71 / 2.65
$\tan\delta$	0.28 / 0.30	0.15 / 0.17	0.24 / 0.29
Density (kg/m^3)	1010	920	1040

Fig. 4. Realized gain (dB) radiation pattern of the proposed implantable antenna vs. polar angle (coordinate system defined in Fig. 2).

and 4.8 GHz, exhibiting a reflection coefficient of -5.4 dB and -10.0 dB, respectively. As noted above, our design optimization criteria related to maximizing the broadside realized gain at 2.4 / 4.8 GHz. That is, minimization of $|S_{11}|$ at the target frequency was not a design criterion on its own, hence the minor detuning. The antenna can In any case, the achieved reflection coefficient is certainly acceptable, indicating that 71.2% (at 2.4 GHz, where |S11|=-5.4 dB) and 90.0% (at 4.8 GHz, where |S11|=-10dB, per Fig. 5) of the energy flows into the antenna. To improve the matching, a feasible alternative could be to include a lumped element matching network. The 10-dB bandwidth across the 2.4 GHz and 4.8 GHz bands is equal to 80 MHz and 115 MHz, respectively.

Specific Absorption Rate (SAR) simulations were also performed for the implantable antenna, as shown in Fig. 6(a) and Fig. 6(b) for 2.4 GHz and 4.8 GHz, respectively. The plots show the SAR averaged over 1 g of tissue (SAR$_{1g}$). It was found that input power levels as high as 4.75 mW at 2.4 GHz
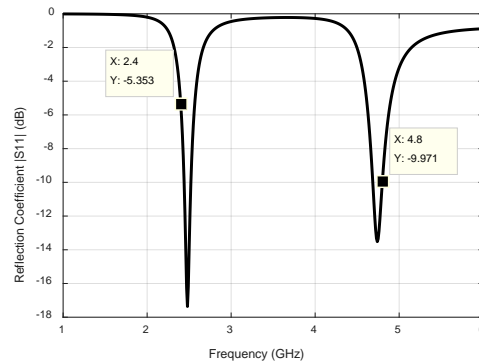

Fig. 5. Simulated antenna reflection coefficient vs. frequency.
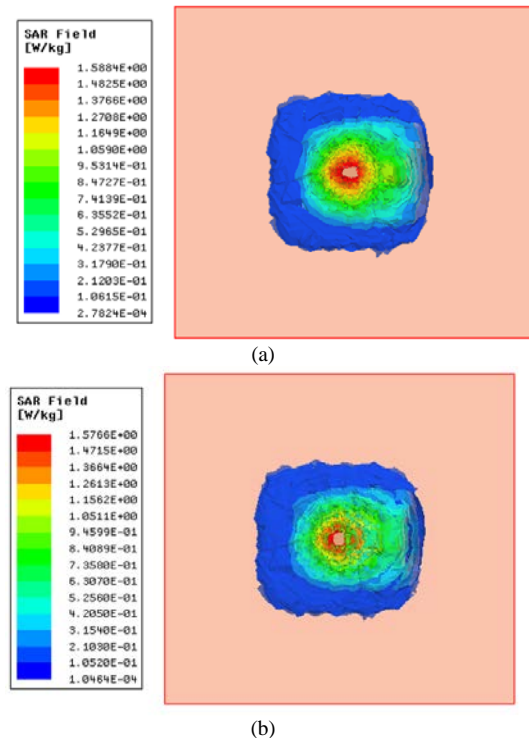

(a)

(b)

Fig. 6. SAR$_{1g}$ simulations at: a) 2.4 GHz (input power = 4.75 mW), and b) 4.8 GHz (input power = 2.80 mW).

and 2.80 mW at 4.8 GHz guarantee conformance with the FCC patient safety guidelines (i.e., SAR$_{1g} \leq$ 1.6 W/kg [24]).

IV. IN VIVO TESTING IN PMHS

A. Measurement Set-Up

For validation, the proposed 2.4/4.8 GHz implantable antenna design was fabricated (see Fig. 1(b)), and further implanted in six (6) locations of a PMHS. The PMHS was a 65 year old male (weight: 78.5 kg; height: 185.4 cm), available through The Ohio State University's Body Donor Program. The PMHS did not have any disease or abnormality on the skin, subcutaneous tissue and muscle. All applicable Body Donor Program and University guidelines were reviewed and followed.

Antenna implantation was performed on the left and right side of three locations: lateral aspect of the mid-thigh over the

Fig. 7. Fresh PMHS with incision locations (thigh, hip, and abdomen) shown on the right side. Similar incisions were performed on the left side.

TABLE IV. MEASURED REFLECTION COEFFICIENT AT RESONANCES IN VARIOUS PMHS LOCATIONS

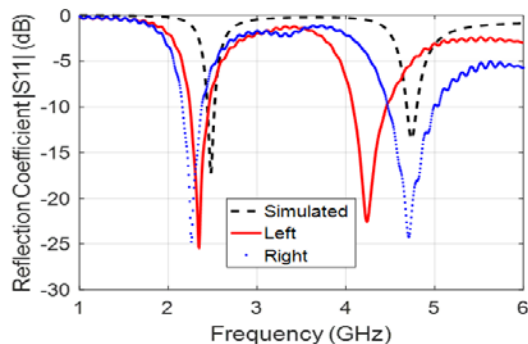| Location	2.4 GHz Band		4.8 GHz Band	
	$|S_{11}|$ (dB)	BW (MHz)	$|S_{11}|$ (dB)	BW (MHz)
Left Thigh	-14.3	212	-4.5	372
Right Thigh	-8.8	218	-18.5	513
Left hip	-9.8	242	-19.9	584
Right hip	-5.4	224	-8.8	472
Left Abdomen	-8.4	260	-7.9	343
Right Abdomen	-13.5	236	-12.5	360
Simulations	-5.4	81	-10	115

Fig. 8.   Simulated vs. measured reflection coefficient ($|S_{11}|$) of the implantable antenna inside of the PMHS thigh.
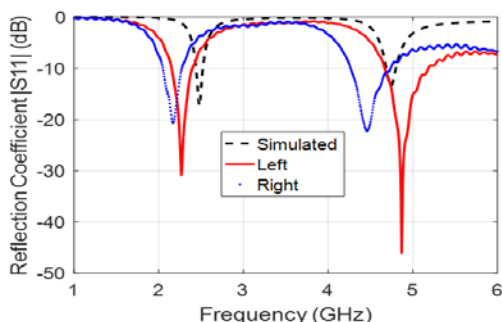

Fig. 9.   Simulated vs. measured reflection coefficient ($|S_{11}|$) of the implantable antenna inside of the PMHS hip.
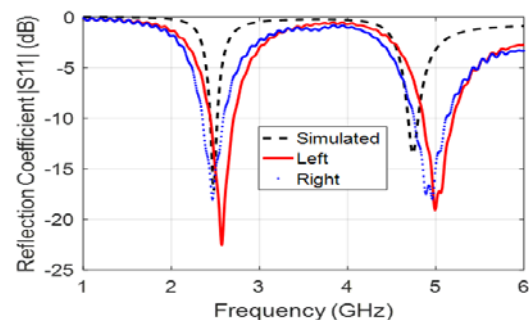

Fig. 10.   Simulated vs. measured reflection coefficient ($|S_{11}|$) of the implantable antenna inside of the PMHS abdomen.

vastus lateralis muscle, lateral aspect of the hip over the gluteus maximus muscle at the level of the greater trochanter, and anterolateral aspect of abdomen over the external oblique muscle approximately 25.4 mm above umbilicus, as shown by Fig. 7. Measurements of the antenna's reflection coefficient ($|S_{11}|$) were conducted with a FieldFox Handheld VNA.

B.   Measurement Results

The measured reflection coefficient performance in the thigh, glute and abdomen is shown in Figs. 8-10, and further super-imposed with simulation results for the 3-layer tissue model of Fig. 2. As seen, the antenna is matched most closely in the abdomen, possibly due to the tightness of the PMHS's skin in that location from lying in the supine position. Variations in the performance at different locations can most likely be attributed to the differences in skin thicknesses and/or minor variations in the incision formation of the subcutaneous "pockets".

Table IV provides quantitative data of the measured reflection coefficient magnitude at 2.4/4.8 GHz and the respective bandwidths. Simulation results from Fig. 4 are also included for completeness. As seen, the best matched measurement to the 2.4/4.8 GHz resonance goal is the right abdomen with both resonances being below -10 dB. The worst matched resonance is the 4.8 GHz in the left thigh, which only has a -4.5 dB reflection coefficient. The antenna bandwidth increases as compared to simulation, showing that the PMHS is lossier than the simulation model. Notably, a reflection coefficient of < -4.5 dB is measured at both 2.4 and 4.8 GHz for all six subcutaneous locations. This implies that at least 64.5% of the provided energy flows into the antenna in all cases.

V.   CONCLUSION

In this paper, we proposed a novel miniaturized 2.4/4.8 GHz implantable antenna and verified its performance through simulations and PMHS testing. Compared to the smallest implantable antenna operating in the same bands [6], the proposed design exhibits: a) 39% smaller footprint, and b) higher realized gain by 10.3 dB (at 2.4 GHz) and 2.6 dB (at 4.8 GHz). PMHS testing was in good agreement with simulated results. Certain detuning was measured, as attributed to variations in anatomy, skin thickness, and surgical incision procedure. Nevertheless, a reflection coefficient of < -4.5 dB was measured in all cases implying that at least 64.5% of the provided energy flows into the antenna.

REFERENCES

[1]   V. Ranganathan, et al, "A high-voltage compliant neural simulator with HF wireless power and UHF backscatter communication," in Proc. Wireless Power Transfer Conference, May 2016.

[2] P. Anacleto, P. M. Mendes, E. Gultepe, and D. H. Gracias, "3D small antenna for energy harvesting applications on implantable micro-devices," in Proc. 2012 Loughborough Antennas & Propagaion Conference, Nov. 2012.

[3] C. Poon, B. Lo, M. Rasit Yuce, A. Alomainy and Y. Hao, "Body Sensor Networks: In the Era of Big Data and Beyond," IEEE Reviews in Biomedical Engineering, vol. 8, pp. 4-16, April 2015.

[4] C.W. L. Lee et al., "A high-sensitivity fully-passive neurosensing system for wireless brain signal monitoring," IEEE Trans. Microw. Theory Tech.,vol. 63, no. 6, pp. 2060–2068, Jun. 2015.

[5] A. Kiourti et al., "A Wireless Fully Passive Neural Recording Device for Unobtrusive Neuropotential Monitoring," IEEE Trans. Biomedical Engineering, vol. 63, no. 1, pp 131-137, Jan. 2016.

[6] C. W. L. Lee et al., "Miniaturized Fully Passive Brain Implant for Wireless Neuropotential Acquisition," IEEE Antennas and Wireless Propagation Letters, vol. 16, pp. 645-648, Mar. 2017.

[7] Y. Liu, Y. Chen, H. Lin, and F. Juwono, "A novel differentially fed compact dual-band implantable antenna for biotelemetry applications," IEEE Antennas and Wireless Propagation Letters, vol. 15, pp. 1791-1794, Mar. 2016.

[8] Y. Cho and H. Yoo, "Miniaturized dual-band implantable antenna for wireless biotelemetry," Electronics Letters, vol. 52, iss. 12, pp. 1005-1007, Jun. 2016.

[9] S. Shah and H. Yoo, "Scalp-implantable antenna systems for intracranial pressure monitoring," IEEE Trans. Antennas and Propagation, vol. 66, iss. 4, pp. 2170-2173. Apr. 2018.

[10] A. RamRakhyani and G. Lazzi, "On the design of efficient multi-coil telemetry system for biomedical implants," IEEE Transacations on Biomedical Circuits and Systems, vol. 7, iss. 1, pp. 11-23, Feb. 2013.

[11] E. Moradi et al., "Backscattering neural tags for wireless brain-machine interface systems," IEEE Trans. Antennas and Propagation, vol. 63, iss. 2, pp.719-726, Dec. 2014.

[12] M. Manoufali, K. Bialkowski, B. Mohammed, P. Mills and A. Abbosh, "Near-Field Inductive-Coupling Link to Power a Three-Dimensional Millimeter-Size Antenna for Brain Implantable Medical Devices," IEEE Transactions on Biomedical Engineering, vol. 65, iss.1, pp. 4-14, Jan. 2018.

[13] A. Alemaryeen and S. Noghanian, "Crumpling effects and specific absorption rates of flexible AMC integrated antennas," IET Microwaves, Antennas, & Propagation, vol. 2, iss. 4, pp. 627-635, Mar. 2018.

[14] H. Bahrami et. al., "Flexible, Polarization-Diverse UWB Antennas for Implantable Neural Recording Systems," IEEE Transactions on Biomedical Circuits and Systems, vol. 10, no. 1, pp. 38-48, Feb. 2016.

[15] M. Magill, G. Conway and W. Scanlon, "Tissue-Independent Implantable Antenna for In-Body Communications at 2.36–2.5 GHz," IEEE Transactions on Antenans and Propagation, vol. 65, no. 9, Sep. 2017.

[16] T. Karacolak, R. Cooper, E. Unlu and E. Topsakal, "Dielectric properties of porcine skin tissue and in vivo testing of implantable antennas using pigs as model animals," IEEE Antennas and Wireless Propagation Letters, vol. 11, pp. 1686-1689, 2012.

[17] A. Kiourti and K. Nikita, "Accelerated design of optimized implantable antennas for medical telemetry," IEEE Antennas and Wireless Propagation Letters, vol.11, pp. 1655-1658, 2012.

[18] K. Bocan, M. Mickle and E. Sejdic, "Tissue Variability and Antennas for Power Transfer to Wireless Implantable Medical Devices," IEEE Journal of Translational Engineering in Health and Medicine, vol. 5, Aug. 2017.

[19] OET Bulletin.65, 1997. "ITU-R Radio Regulations section 5.138 and 5.150," Int. Telecommun. Union-Radiocommun., Geneva, Switzerland.

[20] A. Kiourti and K. Nikita, "A Review of Implantable Patch Antennas for Biomedical Telemetry: Challenges and Solutions,"IEEE Antennas and Propagation Magazine, vol. 54, iss. 3, pp. 210-218, June 2012.

[21] S. Koulouridis, G. Kiziltas, Y. Zhou, D. J. Hansford, and J. L. Volakis, "Polymer-ceramic composites for microwave applications: Fabrication and performance assessment," IEEE Microw. Theory Techn., vol. 54, no. 12, pp. 4202–4208, Dec. 2006.

[22] C. Gabriel, "Compilation of the dielectric properties of body tissues at RF and microwave frequencies," Report N.AL/OE-TR- 1996-0037, Occupational and environmental health directorate, Radiofrequency Radiation Division, Brooks Air Force Base, Texas (USA), June 1996.

[23] J. Kim and Y. Rahmat-Samii, "Implanted antennas inside a human body: simulations, designs, and characterizations," IEEE Transactions on Microwave Theory and Techniques, vol. 52, iss. 8, pp. 1934 – 1943, Aug. 2004.

[24] "Evaluating compliance with FCC guidelines for human exposure to radio frequency electromagnetic fields," FCC, Washington, DC, USA.